


## Dissipative dynamics of an impurity with spin-orbit coupling

Areg Ghazaryan, Alberto Cappellaro , Mikhail Lemeshko, and Artem G. Volosniev   
*Institute of Science and Technology Austria (ISTA), am Campus 1, 3400 Klosterneuburg, Austria*

 (Received 17 October 2022; accepted 19 December 2022; published 20 January 2023)

Brownian motion of a mobile impurity in a bath is affected by spin-orbit coupling (SOC). Here, we discuss a Caldeira-Leggett-type model that can be used to propose and interpret quantum simulators of this problem in cold Bose gases. First, we derive a master equation that describes the model and explore it in a one-dimensional (1D) setting. To validate the standard assumptions needed for our derivation, we analyze available experimental data without SOC; as a byproduct, this analysis suggests that the quench dynamics of the impurity is beyond the 1D Bose-polaron approach at temperatures currently accessible in a cold-atom laboratory—motion of the impurity is mainly driven by dissipation. For systems with SOC, we demonstrate that 1D spin-orbit coupling can be gauged out even in the presence of dissipation—the information about SOC is incorporated in the initial conditions. Observables sensitive to this information (such as spin densities) can be used to study formation of steady spin polarization domains during quench dynamics.

DOI: [10.1103/PhysRevResearch.5.013029](https://doi.org/10.1103/PhysRevResearch.5.013029)

### I. INTRODUCTION

Dissipation of energy occurs naturally when a particle with finite momentum moves through a medium. This phenomenon is typically studied assuming that the momentum of the particle is decoupled from its spin degree of freedom. This is, however, not the case for many condensed matter systems with strong spin-orbit coupling (SOC), in particular, for externally driven setups with nontrivial topological character, such as bosonic Kitaev-Majorana chains [1,2], Majorana wires [3,4], as well as systems featuring optical spin-Hall effect [5,6]. SOC is also key for explaining transport of electrons through a layer of chiral molecules [7,8]. To understand equilibration processes in these systems and promote their use in technologies, studies of dissipative dynamics with SOC are needed. Cold-atom-based quantum simulators provide a natural test bed for such studies [9,10]—they complement the existing research of out-of-equilibrium time evolution, see, e.g., Refs. [11–13], and SOC engineering using laser fields [14,15].

To enjoy the potential of quantum simulators, one requires theoretical models that can be used to propose new experiments and analyze the existing data [16]. In this paper, we present one such model designed to study an impurity with SOC (see also recent Ref. [17] for a discussion of a relevant Langevin-type equation). The impurity is in contact with the bath that we model as a collection of harmonic oscillators. Using the Born and Markov approximations, we derive a master equation, which extends the result of Caldeira and

Leggett [18,19] to a spin-orbit-coupled impurity. To illustrate this equation, we focus on one-dimensional (1D) systems. First, we test it using the experimental data of Ref. [20], whose full theoretical understanding is lacking, see, e.g., Ref. [21]. We find that the Caldeira-Leggett model contains all ingredients to describe the observed breathing dynamics of the impurity assuming that the initial condition is the (only) tunable parameter. The calculations are *analytical*, which simplifies the analysis and allows us to gain insight into the system: relevant timescales, short- and long-time dynamics. Finally, we explore the dynamics of the system with SOC. Without magnetic fields, the 1D SOC can be gauged out so the system can be described using the Caldeira-Leggett equation with SOC-dependent initial conditions. We present observables that are sensitive to these initial conditions and can be used to study the effect of SOC on time dynamics, for example, formation of regions with steady spin polarization. Our findings provide a convenient theoretical model that can be used to propose and benchmark quantum simulators of dissipative dynamics with SOC.

### II. THE PARTICLE-BATH HAMILTONIAN

The Hamiltonian of the system is given by  $H_{\text{tot}} = H_S + H_B + H_C$ . The three terms account for, correspondingly, the (quantum) impurity, the harmonic bath, and the bath-impurity coupling. We assume that  $H_S$  has the form

$$H_S = \frac{\mathbf{p}^2}{2m} + V_{\text{SO}}(\mathbf{p}, \sigma) + \mathcal{V}_{\text{ext}}(\mathbf{q}) + \mathbf{q}^2 \sum_{j=1}^N \frac{c_j^2}{2m_j \omega_j^2}, \quad (1)$$

where  $m$  and  $\mathbf{q}$  are the mass and the position of the impurity, respectively.  $\mathcal{V}_{\text{ext}}$  is an external potential.  $V_{\text{SO}}(\mathbf{p}, \sigma)$  is the potential that describes SOC; it depends on the Pauli vector,  $\sigma$ , and the momentum of the impurity,  $\mathbf{p}$ . A particular form of  $V_{\text{SO}}$  is specified below, see also Appendix A 6. The last term in

*Published by the American Physical Society under the terms of the Creative Commons Attribution 4.0 International license. Further distribution of this work must maintain attribution to the author(s) and the published article's title, journal citation, and DOI.*

Eq. (1) is a standard harmonic counterterm, which makes  $H_{\text{tot}}$  translationally invariant for  $\mathcal{V}_{\text{ext}} = 0$  [22]. The parameters  $\omega_j$  and  $m_j$  are taken from the bath Hamiltonian,

$$H_B = \sum_j \left[ \frac{\mathbf{p}_j^2}{2m_j} + \frac{1}{2} m_j \omega_j^2 \mathbf{x}_j^2 \right], \quad (2)$$

whereas  $c_j$  enters the bath-impurity interaction

$$H_C = -\mathbf{q} \cdot \sum_j c_j \mathbf{x}_j. \quad (3)$$

For microscopic derivations that validate the form of  $H_B$  and  $H_C$  for weakly interacting Bose gases and Luttinger liquids, see, correspondingly, Refs. [23,24].

To summarize, we consider a single particle (impurity) linearly coupled to an environment made of noninteracting harmonic oscillators using the standard procedure [18,25], briefly outlined below; this well-studied problem is extended here by subjecting the impurity to SOC.

Before analyzing  $H_{\text{tot}}$ , we remark that there are a number of theoretical methods [26–30] that can be used for interpreting experiments with impurities in Fermi [31–34] and Bose gases [20,35–39]. Time evolution of an impurity in a Bose gas—the focus of this paper—has been studied using variational wave functions,  $T$ -matrix approximations, and exact solutions in 3D at zero [40–42] and finite temperatures [43]. Many more methods exist to address the 1D world. For example, experimentally relevant trapped systems can be studied using numerically exact approaches [44,45], for a review, see Ref. [46]. In cases when those methods do not work (e.g., large energy exchange or high temperature), it has been suggested to connect a cold-atom impurity to quantum Brownian motion [23,47–49]. Our work provides an example of when this idea leads to an accurate description of experimental data, setting the stage for testing assumptions behind theoretical models of relaxation [19,22] in a cold-atom laboratory.

### III. BORN-MARKOV MASTER EQUATION WITH SOC

Time evolution of the impurity-bath ensemble, defined by  $H_{\text{tot}}$ , obeys the von Neumann equation:  $i\hbar\dot{\rho}_{\text{tot}} = [H_{\text{tot}}, \rho_{\text{tot}}]$ . To extract dynamics of the impurity from  $\rho_{\text{tot}}$ , we rely on the Born-Markov approximation [19,50,51], which leads to the equation for the (reduced) density matrix that describes the impurity,  $\rho_S$ :

$$\begin{aligned} \frac{d\rho_S}{dt} = & -\frac{i}{\hbar}[H_S, \rho_S] - \frac{1}{\hbar^2} \int_0^{+\infty} ds \mathcal{C}(s)[\mathbf{q}, [\mathbf{Q}(-s), \rho_S]] \\ & + \frac{i}{\hbar^2} \int_0^{+\infty} ds \chi(s)[\mathbf{q}, \{\mathbf{Q}(-s), \rho_S\}]. \end{aligned} \quad (4)$$

We write Eq. (4) in the form standard for a Brownian particle; the contribution of SOC is conveniently hidden in  $\mathbf{Q}(t)$ , which is defined as

$$\mathbf{Q}(t) = \frac{i}{\hbar}[H_S, \mathbf{q}] = \mathbf{q} - \left( \frac{\mathbf{p}}{m} + \mathbf{v}_{\text{SO}}(\sigma) \right) t, \quad (5)$$

where  $\mathbf{v}_{\text{SO}} = \partial_{\mathbf{p}} V_{\text{SO}}$  is the contribution to the velocity of the particle due to SOC. Equation (4) contains the bath autocorrelation functions  $\mathcal{C}(t)$  and  $\chi(t)$  in Eq. (4),

$$\begin{aligned} \mathcal{C}(t) &= \hbar \int_0^{+\infty} d\omega J(\omega) \coth\left(\frac{\beta\hbar\omega}{2}\right) \cos(\omega t), \\ \chi(t) &= \hbar \int_0^{+\infty} d\omega J(\omega) \sin(\omega t), \end{aligned} \quad (6)$$

where  $\beta = 1/k_B T$  ( $T$  for temperature and  $k_B$  is the Boltzmann constant). These functions assume that all relevant microscopic information is encoded in the spectral function  $J(\omega)$ , formally defined as  $J(\omega) = \sum_j c_j^2 \delta(\omega - \omega_j)/(2m_j \omega_j)$ . We choose

$$J(\omega) = \frac{2m\gamma}{\pi} \frac{\omega \Omega_c^2}{\Omega_c^2 + \omega^2}, \quad (7)$$

recovering Ohmic dissipation at  $\omega \rightarrow 0$ . The phenomenological parameter  $\Omega_c$  defines the high-frequency behavior of Eq. (7).

The Ohmic spectral density is a standard choice in mesoscopic [19,52,53] and in cold-atom physics [24,54,55]. We employ it here because it leads to a local-in-time damping that agrees with the experimental data used below to validate the model (see also Refs. [24,56] for additional details about Ohmic dissipation in 1D based upon long-wavelength approximations for superfluids). Super-Ohmic dissipation whose relevance for Bose polarons is highlighted in Refs. [23,48] leads to strong memory effects (nonlocal-in-time damping), thus, we do not consider it here.

Using Eqs. (5) and (6), we derive the master equation

$$\begin{aligned} \frac{d\rho_S}{dt} = & -\frac{i}{\hbar}[H_S, \rho_S] - \frac{i\gamma}{\hbar} [\mathbf{q}, \{\mathbf{p}, \rho_S\}] - \frac{2m\gamma}{\beta\hbar^2} [\mathbf{q}, [\mathbf{q}, \rho_S]] \\ & - im\gamma [\mathbf{q}, \{\mathbf{v}_{\text{SO}}, \rho_S\}], \end{aligned} \quad (8)$$

where  $\gamma$  defines the strength of dissipation. Technical details behind the derivation of Eq. (8) are discussed in Appendix A. As expected, dissipative dynamics is affected by SOC, see the last term in Eq. (8). Finally, a proper Lindblad form for Eq. (8) can be achieved by adding a *minimally invasive* term:  $-\gamma\beta[\mathbf{p}[\mathbf{p}, \rho_S]]/(8m)$  [19,57]; we employ this term in our calculations.

To illustrate the master equation, we choose to consider a 1D setting parameterized by the coordinate  $y$ . Without loss of generality, we write the SOC term as  $V_{\text{SO}} = \alpha\sigma_x p_y$ . In this case, the master equation reads as

$$\frac{d\rho}{dt} = \frac{d\rho}{dt} \Big|_{\alpha=0} - \alpha \mathcal{F}[\rho], \quad (9)$$

where  $\mathcal{F}[\rho] = \sigma_x \partial_y \rho + \partial_y \rho \sigma_x + \frac{im\gamma}{\hbar} (y - y')(\sigma_x \rho + \rho \sigma_x)$  with  $\rho \equiv \langle y | \rho_S | y' \rangle$ , and  $\frac{d\rho}{dt} \Big|_{\alpha=0}$  describes time evolution of the system without SOC, see Appendix A 7. The effect of SOC is encoded in  $\alpha \mathcal{F}[\rho]$ .

While the technical details leading to Eq. (4) are presented in Appendix A, we recall here the standard assumptions behind the Born-Markov approximation. First, the impurity-bath density matrix is separable throughout time evolution, such that  $\rho_{\text{tot}}(t) \simeq \rho_S(t) \otimes \rho_B(t)$ . Second, the bath is not

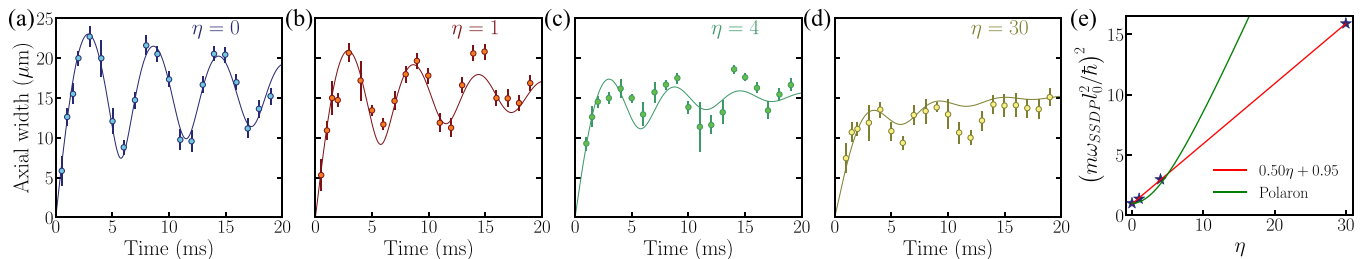


FIG. 1. (a)–(d) The width of the impurity (potassium) cloud  $\bar{y}$  as a function of time for different values of the parameter  $\eta$ . The dots with error bars show the experimental data of Ref. [20]. The curves are the fits to Eq. (9). Panel (e) shows the values of  $l_0$  used in the fit as a function of  $\eta$ . The panel also shows a linear fit to these values (red line). The green curve shows the effective mass of the polaron calculated using the analytical methods outlined in Refs. [58,59] (no fitting parameters).

affected by the impurity motion, namely,  $\rho_B(t) \simeq \rho_B^{\text{eq}}$ . This assumption is natural if the decay of bath correlations has the fastest timescale  $\tau_B$ ; it implies that dynamical features  $\sim \tau_B$  are not resolved by our approach [19,50]. To validate these approximations, we shall demonstrate that the master equation is capable of describing experimental data of Ref. [20] that provide a benchmark point for us at  $\alpha = 0$ .

#### IV. DYNAMICS WITHOUT SOC

First, we briefly outline the main features and findings of the experiment of Ref. [20]. In that paper, a potassium atom was used to model an impurity in a gas of rubidium atoms. At  $t = 0$ , the impurity was trapped in a tight trap created by a species-selective dipole potential (SSDP) with  $\omega_{\text{SSDP}}/(2\pi) = 1\text{kHz}$ . At  $t > 0$ , the dynamics was initiated by an abrupt removal of the SSDP; the impurity was still confined by a shallow parabolic potential, i.e.,  $\mathcal{V}_{\text{ext}}(y) = \hbar^2 y^2 / 2ml^4$ , where  $l = \sqrt{\hbar/m\omega}$  and  $\omega = (87 \times 2\pi)\text{Hz}$  is the frequency of the oscillator. The experiment recorded the size of the impurity cloud  $\bar{y} = \sqrt{\langle y^2 \rangle}$ , and found that it can be fit using the expression

$$\bar{y} = \bar{y}_0 + \mathcal{A}_1 t - \mathcal{A}_2 e^{-\Gamma\Omega t} \cos[\sqrt{1 - \Gamma^2\Omega}(t - t_0)], \quad (10)$$

where  $\mathcal{A}_1$ ,  $\mathcal{A}_2$ ,  $\Omega$ ,  $\Gamma$ ,  $\bar{y}_0$ ,  $t_0$  are fitting parameters. The key experimental findings of Ref. [20] were (a)  $\Omega$  (almost) does not depend on the impurity-boson interaction parametrized by  $\eta$ ; (b) by increasing  $\eta$  one decreases the amplitude of the first oscillation; and (c) at long times,  $\bar{y}$  equilibrates to about the same value, which is independent of  $\eta$ . Point (b) was attributed to renormalization of the mass of the impurity, i.e., to a polaron formation [60]. However, this posed several theoretical problems. In particular, the breathing frequency of the polaron cloud should depend on  $\eta$ , which contradicts observation (a), see also discussions in Refs. [20,21,58,61]. Our results below suggest that one can understand the data of Ref. [20] from the perspective of dissipative dynamics.

Equation (9) leads naturally to the dynamics observed in the experiment. To show this, we assume that the initial density matrix of the impurity corresponds to a Gaussian wave

packet

$$\rho(y, y', t = 0) = \frac{1}{\sqrt{\pi}l_0} e^{-\frac{y^2 + y'^2}{2l_0^2}}, \quad (11)$$

where  $l_0$  is the parameter that determines the initial distribution of the impurity momenta; Eq. (11) is standard for particles whose initial state is not precisely known. We calculate the time dynamics for this initial condition analytically using the method of characteristics (see Appendix B 1 and Ref. [62]), which discovers characteristic curves where the master equation can be written as a family of ordinary differential equations [63]. The computed functional dependence resembles Eq. (10) with  $\Gamma\Omega = 2\gamma$ , see Appendix B 2. Note that our calculations have only two phenomenological parameters,  $\gamma$  and  $l_0$ . All other parameters that appear in Eq. (10), i.e.,  $\mathcal{A}_1$ ,  $\mathcal{A}_2$ ,  $\bar{y}_0$ ,  $t_0$ , and  $\Omega$ , can be extracted from our results. For example,  $\Omega \simeq 2\omega$  as in the experiment.

We present analytical results of the master equation together with the experimental data in Fig. 1. The value of  $\gamma$  is restricted to be within the error bars of the experimentally measured value of  $\Gamma\Omega$  (so  $\gamma \sim 40\text{Hz}$ ) [64]. The temperature is set to the value reported in the experiment, i.e.,  $T = 350\text{nK}$  [65]. The quality of the fits in Fig. 1 is comparable to what can be obtained with Eq. (10), allowing us to conclude that the master equation provides a valuable tool for analyzing these data, and cold-atom systems in general.

Let us briefly discuss implications of our results for interpretation of the experiment of Ref. [20]. First, the weak dependence of  $\Omega$  on  $\eta$  is natural in our model: the renormalization of the frequency is given by  $\omega_{\text{eff}} \simeq \omega(1 - \gamma^2/(2\omega^2))$ , where  $\gamma/\omega$  is a small parameter as in the experiment. Second, the parameter  $\bar{y}$  for  $t \rightarrow \infty$  is independent of  $\gamma$  assuming that the thermal de Broglie wavelength is small. Indeed, in this case, we derive  $\bar{y} \simeq \sqrt{k_B T / (\hbar\omega)l} \approx 15.42\mu\text{m}$  in agreement with the measurement.

The amplitude of the first oscillation is determined in our analysis by the initial condition, i.e.,  $l_0$ . To explain values of  $l_0$  obtained in our fit, one can speculate that the impurity forms a polaron state at  $t < 0$  and that at  $t > 0$  the dynamics is dominated by finite-temperature effects. In this picture, the mass of the impurity is renormalized (i.e.,  $m \rightarrow m_p$ ) only before the quench dynamics [66]; this might explain why theoretical

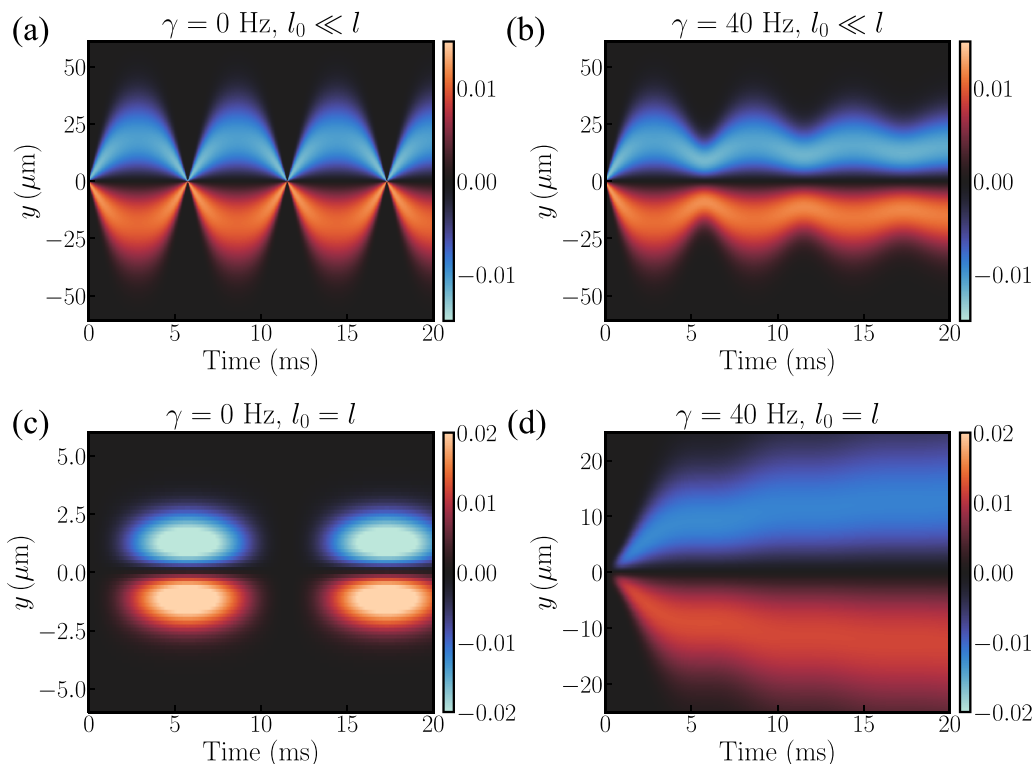


FIG. 2. The spin polarization along the  $y$  axis as a function of position and time in the presence of SOC. The SOC amplitude is  $\alpha = 40 \text{ Hz} \cdot \mu\text{m}$ .  $l_0$  for (a), (b) case corresponds to  $\omega_0/2\pi = 30 \text{ kHz}$ , while  $l$  is given by  $\omega/2\pi = 87 \text{ Hz}$ . All other parameters are as in Ref. [20], in particular,  $T = 350 \text{ nK}$ .

calculations can produce features of the amplitude but not of the frequency [20,21,61]. Renormalization of the mass implies that the energy scale at  $t = 0$  is given by  $\hbar\omega_{\text{SSDP}}\sqrt{m/m_p}$ , which is incorporated into Eq. (11) if [67]

$$l_0^2 \sim \frac{\hbar}{m\omega_{\text{SSDP}}}\sqrt{\frac{m_p}{m}}. \quad (12)$$

This expression agrees qualitatively with the outcome of our fit, see Fig. 1(e). The linear increase of  $(m\omega_{\text{SSDP}}l_0^2/\hbar)^2$ , however, quantitatively disagrees with calculations of the effective mass [21,58,68,69]. The agreement improves if we disregard the point with  $\eta = 30$ , which (as suggested in Ref. [20]) is already beyond a simple 1D treatment [70]. In any case, a further analysis of the experimental data (beyond the scope of this paper) is needed in light of our results.

Finally, we note that the inhomogeneity of the bath as well as non-Markovian physics do not appear to be important to describe dynamics discussed here. This stands in contrast to what is known about properties of the corresponding ground state [71] and low-energy dynamics [58,61,72], and results from a high temperature and large energy ( $\sim 1/l_0^2$ ) associated with the initial impurity state.

## V. DYNAMICS WITH SOC

We use the experimental protocol of Ref. [20] also to illustrate the master equation with SOC. The peculiarity of 1D is that the  $\alpha$ -dependent term can be gauged out from Eq. (9)

via the transformation (in the position space)

$$\rho(y, y', t) = e^{-\frac{i\alpha\sigma_y y}{\hbar}} f(y, y', t) e^{\frac{i\alpha\sigma_y y'}{\hbar}}. \quad (13)$$

The function  $f(y, y', t)$  then satisfies the standard Caldeira-Leggett equation and can be solved exactly as without SOC, see Appendix B 3. Note that the equation for  $f$  is spin independent. The initial condition of the problem,  $\rho(y, y', t = 0)$ , defines the full spin structure of the problem and time dependence of spin observables, as we illustrate below for  $\bar{\sigma}_y(y, t) \equiv \text{Tr}_{\text{spin}}(\sigma_y)$ .

For the sake of discussion, as the initial condition we consider the state that is spin polarized along the  $z$  axis,

$$\rho(y, y', 0) = \frac{1}{2\sqrt{\pi}l_0} e^{-\frac{y^2+y'^2}{2l_0^2}} |\uparrow\rangle\langle\uparrow|; \quad (14)$$

other parameters of the system are taken from Ref. [20]. We use  $\gamma = 40 \text{ Hz}$ , which was typical in that experiment. The strength of SOC,  $\alpha$ , can be tuned in cold-atom setups, see, e.g., Refs. [73–75]. We assume that  $\alpha\bar{y}/(\omega l^2) \ll 1$  to demonstrate that even weak SOC can lead to an observable effect in dynamics.

Time evolution of  $\bar{\sigma}_y(y, t)$  is shown in Fig. 2. Note that Eq. (14) is not an eigenstate of the system with SOC—dynamics occurs even without a change of the trap, i.e.,  $l_0 = l$  [see Figs. 2(c) and 2(d)]. Without dissipation ( $\gamma = 0$ ), we observe oscillation of the spin density with  $\bar{\sigma}_y > 0$  for  $y > 0$  and  $\bar{\sigma}_y < 0$  for  $y < 0$  [see Figs. 2(a) and 2(c)]. This effect is solely due to SOC, and can be easily understood from a

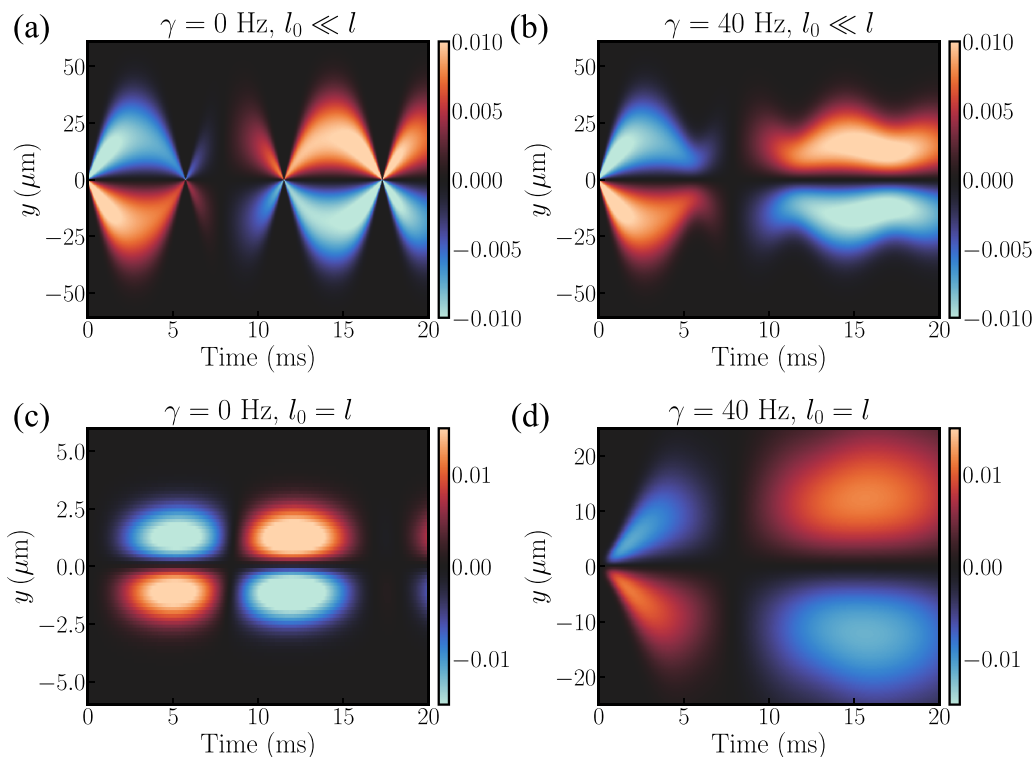


FIG. 3. The same as in Fig. 2 but with an additional magnetic field along the  $y$  direction. The amplitude of the magnetic field is  $\mu_B B/\hbar = 100$  Hz.

one-body Schrödinger equation. Effects of temperature and dissipation are most visible in Fig. 2(d): the impurity is heated by the presence of the bath, which creates regions with steady spin polarization along the  $y$  direction. Spatial extension of these regions is determined by the temperature; the timescale for their formation is given by  $1/\gamma$  (similarly to the dynamics without SOC, see Fig. 1). This effect can be observed in cold-atom systems by analyzing populations of the involved hyperfine states.

Finally, we remark that Eq. (8) allows us to include Zeeman-type terms, which naturally appear in ultracold atoms with synthetic SOC [14,15]. To this end, we add the term  $\mu_B \mathbf{B} \cdot \boldsymbol{\sigma}$  to  $H_S$ . Its presence strongly modifies the spin dynamics because SOC cannot be gauged out. Theoretical analysis also becomes more involved, since we cannot solve the system analytically for all values of  $\alpha$  and  $B$ . Still, we obtain closed-form expressions using tools of perturbation theory for  $\alpha \rightarrow 0$ , see Appendix B 4. The effect of the magnetic field is illustrated in Fig. 3. Initially, the dynamics with the magnetic field is similar to the dynamics presented in Fig. 2. However, at later times we observe spin precession possible only in the presence of both SOC and the magnetic field. Spin precession leads to an exchange of domains with positive and negative values of  $\bar{\sigma}_y$ , and can be used for engineering the spin structure.

## VI. CONCLUSIONS

We analyzed Brownian-type motion of a spin-orbit coupled impurity with the goal to develop a simple theoretical tool that can be used to propose and analyze cold-atom-based

quantum simulators. We introduced a master equation suitable for the problem. We tested it and illustrated its usefulness by interpreting available experimental data without SOC [20]. Our results suggested that the impurity does not experience any mass renormalization during quench dynamics at experimentally accessible temperatures. Finally, we demonstrated that systems with SOC can be studied analytically, and calculated observables that measure changes in population of the hyperfine states of the impurity atom.

A comparison between results of our theoretical study and experimental data (when available) can be used to understand the limits of applicability of a set of assumptions standard for studies of Brownian motion, such as the Markov approximation. In addition, our findings pave the way for studies of various condensed matter systems where SOC and dissipation play a role. For example, models of the chirality induced spin selectivity (CISS) effect [7,8] are typically based upon nonunitary time evolution (e.g., due to dissipation) and SOC, see, e.g., Refs. [76–81]. These effects are included in our model, hence, it can be developed into a testbed for studying CISS [82].

## ACKNOWLEDGMENTS

We thank Rafael Barfknecht for help at the initial stages of this project; Fabian Brauneis for useful discussions; Miguel A. Garcia-March, Georgios Koutentakis, and Simeon Mistakidis for comments on the paper. M.L. acknowledges support by the European Research Council (ERC) Starting Grant No. 801770 (ANGULON).

## APPENDIX A: TECHNICAL DETAILS FOR DERIVATIONS OF THE MASTER EQUATION

### 1. Preliminaries

We start by writing  $H_B$  and  $H_C$  as

$$H_B = \sum_{j=1}^N \left[ \frac{\mathbf{p}_j^2}{2m_j} + \frac{1}{2} m_j \omega_j^2 \mathbf{x}_j^2 \right] = \sum_{j=1}^N \hbar \omega_j \mathbf{b}_j^\dagger \mathbf{b}_j \quad (\text{A1})$$

and

$$H_C = -\mathbf{q} \cdot \sum_{j=1}^N c_j \mathbf{x}_j = -\mathbf{q} \cdot \sum_{j=1}^N c_j \sqrt{\frac{\hbar}{2m_j \omega_j}} (\mathbf{b}_j^\dagger + \mathbf{b}_j), \quad (\text{A2})$$

where  $\mathbf{b}_j^\dagger$  and  $\mathbf{b}_j$  are the standard bosonic creation and annihilation operators, respectively. For convenience, we define the operator

$$\mathcal{B} = \sum_{j=1}^N c_j \sqrt{\frac{\hbar}{2m_j \omega_j}} (\mathbf{b}_j^\dagger + \mathbf{b}_j). \quad (\text{A3})$$

To derive the Born-Markov equation of motion for the impurity, we work in the interaction representation, where  $\mathbf{q}$  and  $\mathcal{B}$  are written as

$$\mathbf{q}(t) = e^{iH_S t/\hbar} \mathbf{q} e^{-iH_S t/\hbar}, \quad \mathcal{B}(t) = e^{iH_B t/\hbar} \mathcal{B} e^{-iH_B t/\hbar} = \sum_{j=1}^N c_j \sqrt{\frac{\hbar}{2m_j \omega_j}} (\mathbf{b}_j e^{-i\omega_j t} + \mathbf{b}_j^\dagger e^{i\omega_j t}). \quad (\text{A4})$$

Here and in what follows, we write explicitly the time dependence [e.g.,  $\mathcal{B} \rightarrow \mathcal{B}(t)$ ] to designate the operators in the interaction representation. The equation of motion for  $\rho_{\text{tot}}$ , namely,  $i\hbar \dot{\rho}_{\text{tot}} = [H_{\text{tot}}, \rho_{\text{tot}}]$ , is formally solved (in the interaction representation) by

$$\rho_{\text{tot}}(t) = \rho_{\text{tot}}(0) - \frac{i}{\hbar} \int_0^t dt' [H_C(t'), \rho_{\text{tot}}(t')]. \quad (\text{A5})$$

Equation (A5) can be iterated one more time, leading to

$$\rho_{\text{tot}}(t) = \rho_{\text{tot}}(0) - \frac{i}{\hbar} \int_0^t dt' [H_C(t'), \rho_{\text{tot}}(0)] - \frac{1}{\hbar^2} \int_0^t dt' \int_0^{t'} dt'' [H_C(t'), [H_C(t''), \rho_{\text{tot}}(t'')]]. \quad (\text{A6})$$

A time derivative of this equation reads

$$\frac{d\rho_{\text{tot}}(t)}{dt} = -\frac{i}{\hbar} [H_C(t), \rho_{\text{tot}}(0)] - \frac{1}{\hbar^2} \int_0^t dt' [H_C(t), [H_C(t'), \rho_{\text{tot}}(t')]]. \quad (\text{A7})$$

### 2. Initial conditions

Let us specify the initial conditions for Eq. (A7). For quench dynamics considered in the main text, we assume that the system is put in contact with the environment at  $t = 0$  such that

$$\rho_{\text{tot}}(0) = \rho_S(0) \otimes \rho_B(0), \quad (\text{A8})$$

where  $\rho_B(0)$  is the equilibrium distribution for the bath and  $\rho_S(0)$  is the density matrix of the impurity. Under this condition, the first term on the right-hand side of Eq. (A7) vanishes when we trace over the degrees of freedom of the bath:

$$\text{Tr}_B [H_C, \rho_S(0) \otimes \rho_B(0)] = \text{Tr}_B [-\mathbf{q} \mathcal{B}, \rho_S(0) \otimes \rho_B(0)] = [-\mathbf{q}, \rho_S(0)] \text{Tr}_B [\mathcal{B}, \rho_B(0)] = [-\mathbf{q}, \rho_S(0)] \langle \mathcal{B} \rangle_{\text{bath}} = 0. \quad (\text{A9})$$

By taking the partial trace,  $\text{Tr}_B$ , over Eq. (A7), we derive

$$\frac{d\rho_S(t)}{dt} = -\frac{1}{\hbar^2} \int_0^t dt' \text{Tr}_B [H_C(t), [H_C(t'), \rho_{\text{tot}}(t')]]. \quad (\text{A10})$$

### 3. The Born-Markov approximation

To deal with  $\rho_{\text{tot}}(t)$  in Eq. (A10), we employ the Born approximation, which assumes that the system-environment coupling is so weak that the bath is (almost) not affected by the dynamical evolution of the system. Technically speaking, it means

$$\rho_{\text{tot}}(t) \simeq \rho_S(t) \otimes \rho_B^{\text{eq}}, \quad (\text{A11})$$

with  $\rho_B^{\text{eq}}$  being the bath density matrix at thermal equilibrium.

To further simplify the model, we adopt the coarse-grained perspective on the time axis. In this Markovian picture, the decay of bath correlations provides the shortest timescale ( $\tau_B$ ); we cannot resolve dynamical features with a comparable characteristic time. This means that we replace  $t' \rightarrow t - t'$  and then let  $\int_0^t dt' \rightarrow \int_0^{+\infty} dt'$ . With these assumptions, Eq. (A10) leads to

$$\frac{d\rho_S(t)}{dt} = -\frac{1}{\hbar^2} \int_0^{+\infty} dt' \text{Tr}_B[H_C(t), [H_C(t-t'), \rho_S(t) \otimes \rho_B^{\text{eq}}]]. \quad (\text{A12})$$

In the Schrödinger representation, the Born-Markov master equation is written as

$$\begin{aligned} \frac{d\rho_S}{dt} &= -\frac{i}{\hbar}[H_S, \rho_S] - \frac{1}{\hbar^2} \int_0^{+\infty} dt' \text{Tr}_B[H_C, [H_C(-t'), \rho_S(t) \otimes \rho_B^{\text{eq}}]] \\ &= -\frac{i}{\hbar}[H_S, \rho_S] - \frac{1}{\hbar^2} \int_0^{+\infty} dt' \mathcal{C}(t')[\mathbf{q}, [\mathbf{Q}(-t'), \rho_S]] + \frac{i}{\hbar^2} \int_0^{+\infty} dt' \chi(t')[\mathbf{q}, \{\mathbf{Q}(-t'), \rho_S\}], \end{aligned} \quad (\text{A13})$$

where  $\mathbf{Q}(t)$  is defined according to Eq. (5) in the main text.

#### 4. Autocorrelation functions

The key quantities in Eq. (A13) are the bath autocorrelation functions  $\mathcal{C}(t)$  and  $\chi(t)$  defined as

$$\begin{aligned} \mathcal{C}(t) &= \frac{1}{2} \sum_{j=1}^N c_j^2 \langle \{\mathbf{x}_j(t), \mathbf{x}_j(0)\} \rangle_B = \hbar \int_0^{+\infty} d\omega J(\omega) \coth\left(\frac{\beta\hbar\omega}{2}\right) \cos(\omega t), \\ \chi(t) &= \frac{i}{2} \sum_{j=1}^N c_j^2 \langle [\mathbf{x}_j(t), \mathbf{x}_j(0)] \rangle_B = \hbar \int_0^{+\infty} d\omega J(\omega) \sin(\omega t); \end{aligned} \quad (\text{A14})$$

they are related to noise and dissipation, respectively. The relation becomes clear by looking at Eq. (A13) and by considering the corrections beyond the (closed-system) Schrödinger dynamics. These corrections are encoded in a superoperator whose real part is proportional to  $[\mathbf{q}, [\mathbf{Q}(-t), \rho_S]]$  with coefficient  $\mathcal{C}(t)$ ; the imaginary part is determined to  $\chi(t)[\mathbf{q}, \{\mathbf{Q}(-t), \rho_S\}]$ .

The spectral function,  $J(\omega)$ , that enters in the autocorrelation functions is formally defined as

$$J(\omega) = \sum_{j=1}^N \frac{c_j^2}{2m_j\omega_j} \delta(\omega - \omega_j). \quad (\text{A15})$$

However, as mentioned in the main text, it is worth moving to the frequency continuum and devise a reasonable, phenomenological choice for  $J(\omega)$ . One possibility (employed in our paper) is

$$J(\omega) = \frac{2m\gamma}{\pi} \omega \frac{\Omega_c^2}{\Omega_c^2 + \omega^2}. \quad (\text{A16})$$

It leads to the standard Ohmic dissipation ( $J(\omega) \sim \omega$ ) at low frequencies. Equation (A16) does not have any abnormal behavior (i.e.,  $J(\omega)$  does not diverge) at high frequencies thanks to the high-frequency cutoff determined by the phenomenological parameter  $\Omega_c$ . This leads to meaningful theoretical results. Using the autocorrelation functions in Eq. (A13), we derive Eq. (8) of the main text.

#### 5. Calculation of integrals

Below we give an example of how the frequency integrals leading to Eq. (8) are computed. By recalling the definition of  $\mathbf{Q}(t)$  in Eq. (5) of the main text, we typically have to deal with

$$-\frac{i}{2m\hbar^2} \int_0^{+\infty} dt' t' \chi(t')[\mathbf{q}, \{\mathbf{p}/m + \mathbf{v}_{\text{SO}}, \rho_S\}] = -\frac{i}{\hbar m} \int_0^{+\infty} d\omega J(\omega) \int_0^{+\infty} dt' t' \sin(\omega t')[\mathbf{q}, \{\mathbf{p}/m + \mathbf{v}_{\text{SO}}, \rho_S\}]. \quad (\text{A17})$$

Now, we notice that the integral over time can be interpreted as a derivative of the Dirac delta function. More precisely,

$$\int_0^{+\infty} dt t \sin(\omega t) = \frac{1}{2} \int_{-\infty}^{+\infty} dt t \sin(\omega t) = -\pi \frac{\partial}{\partial \omega} \int_{-\infty}^{+\infty} \frac{dt}{2\pi} \cos(\omega t) = -\pi \delta'(\omega). \quad (\text{A18})$$

Therefore, we can write Eq. (A17) as

$$\begin{aligned}
 -\frac{i}{\hbar m} \int_0^{+\infty} d\omega J(\omega) \int_0^{+\infty} dt' t' \sin(\omega t') [\mathbf{q}, \{\mathbf{p}/m + \mathbf{v}_{\text{SO}}, \rho_S\}] &= -\frac{i\pi}{2\hbar m} \int_{-\infty}^{+\infty} d\omega \delta(\omega) \partial_\omega J(\omega) [\mathbf{q}, \{\mathbf{p}/m + \mathbf{v}_{\text{SO}}, \rho_S\}] \\
 &= -\frac{i\pi}{2\hbar m} [\lim_{\omega \rightarrow 0^+} J'(\omega)] [\mathbf{q}, \{\mathbf{p}/m + \mathbf{v}_{\text{SO}}, \rho_S\}] \\
 &= -\frac{i\gamma}{\hbar} [\mathbf{q}, \{\mathbf{p}/m + \mathbf{v}_{\text{SO}}, \rho_S\}]. \tag{A19}
 \end{aligned}$$

### 6. Spin-orbit coupling

Depending on the form of the SOC, the velocity operator, defined as  $\mathbf{v}_{\text{SO}} = \partial_{\mathbf{r}} \mathbf{Q}$ , with  $\mathbf{Q}$  as in Eq. (5) in the main text, is given by

$$v_{\text{SO},1D} = \frac{p}{m} + \alpha s \tag{A20}$$

for a strictly 1D setup ( $V_{\text{SO}} = s\alpha p$ ,  $p$  being the particle momentum operator), or

$$\mathbf{v}_{\text{SO},2D} = \frac{\mathbf{p}}{m} \sigma_0 - \frac{\alpha}{\hbar} \sigma_y \mathbf{e}_x + \frac{\alpha}{\hbar} \sigma_x \mathbf{e}_y, \tag{A21}$$

for a two-dimensional Rashba-like coupling, namely,  $V_{\text{SO}} = \alpha(-\sigma_y p_x + \sigma_x p_y)/\hbar$ . The first terms on the right-hand sides of Eqs. (A20) and (A21) represent the standard relation between the momentum and the velocity. The other terms enter due to the presence of SOC.

### 7. Master equation in coordinate space

The general form of the master equation in the presence of SOC is presented in the main text, see Eq. (8). For our calculations, we use this equation in the position-space representation where a 1D setup is described by the equation

$$\begin{aligned}
 \frac{d\rho}{dt} &= \left[ \frac{i\hbar}{2m} (\partial_y^2 - \partial_{y'}^2) - \gamma(y - y') \cdot (\partial_y - \partial_{y'}) - \frac{2m\gamma}{\beta\hbar^2} (y - y')^2 - \frac{i}{\hbar} (\mathcal{V}_{\text{ext}}(y) - \mathcal{V}_{\text{ext}}(y')) \right] \rho \\
 &\quad - \alpha(\sigma_x \partial_y \rho + \partial_{y'} \rho \sigma_x) - \frac{im\gamma\alpha}{\hbar} (y - y')(\sigma_x \rho + \rho \sigma_x) \frac{i\mu_B \mathbf{B}}{\hbar} \cdot (\sigma \rho - \rho \sigma) + \frac{\hbar^2 \gamma \beta}{8m} (\partial_y^2 + \partial_{y'}^2 + 2\partial_y \cdot \partial_{y'}) \rho, \tag{A22}
 \end{aligned}$$

where  $\rho \equiv \langle \mathbf{r} | \rho_S | \mathbf{r}' \rangle$ .

For the sake of completeness, we also present the result for 2D setups:

$$\begin{aligned}
 \frac{d\rho}{dt} &= \left[ \frac{i\hbar}{2m} (\nabla_{\mathbf{r}}^2 - \nabla_{\mathbf{r}'}^2) - \gamma(\mathbf{r} - \mathbf{r}') \cdot (\nabla_{\mathbf{r}} - \nabla_{\mathbf{r}'} - \frac{2m\gamma}{\beta\hbar^2} (\mathbf{r} - \mathbf{r}')^2 - \frac{i}{\hbar} (\mathcal{V}_{\text{ext}}(\mathbf{r}) - \mathcal{V}_{\text{ext}}(\mathbf{r}')) \right] \rho \\
 &\quad - \alpha(\sigma_x \partial_y \rho + \partial_{y'} \rho \sigma_x - \sigma_y \partial_x \rho - \partial_{x'} \rho \sigma_y) - \frac{im\gamma\alpha}{\hbar} [(y - y')(\sigma_x \rho + \rho \sigma_x) - (x - x')(\sigma_y \rho + \rho \sigma_y)] \\
 &\quad - \frac{i\mu_B \mathbf{B}}{\hbar} \cdot (\sigma \rho - \rho \sigma) + \frac{\hbar^2 \gamma \beta}{8m} (\nabla_{\mathbf{r}}^2 + \nabla_{\mathbf{r}'}^2 + 2\nabla_{\mathbf{r}} \cdot \nabla_{\mathbf{r}'}) \rho. \tag{A23}
 \end{aligned}$$

## APPENDIX B: TECHNICAL DETAILS FOR CALCULATIONS WITH THE MASTER EQUATION

### 1. Solution of the 1D master equation with $\alpha = 0$

When  $\alpha = 0$  or  $B = 0$ , the master Eq. (A22) can be solved exactly. Let us analyze these limits before moving to the case when both terms are present. First, we shall concentrate on the system without SOC, i.e.,  $\alpha = 0$  and  $B \neq 0$ . We write the density matrix as  $\rho = \rho_0 \sigma_0 + \rho_1 \sigma_x + \rho_2 \sigma_y + \rho_3 \sigma_z$  and assume (without loss of generality) that  $\mathbf{B} \parallel \mathbf{y}$ . Converting from  $\rho_1$  and  $\rho_3$  into  $\rho_{\pm} = \rho_1 \pm i\rho_3$ , we have the equations

$$\frac{d\rho_j}{dt} = \left[ \frac{i\hbar}{2m} (\partial_y^2 - \partial_{y'}^2) - \gamma(y - y')(\partial_y - \partial_{y'}) - \frac{2m\gamma}{\beta\hbar^2} (y - y')^2 - \frac{i\hbar}{2ml^4} (y^2 - y'^2) - \frac{2is\mu_B B}{\hbar} + \frac{\hbar^2 \gamma \beta}{8m} (\partial_y^2 + \partial_{y'}^2 + 2\partial_y \partial_{y'}) \right] \rho_j, \tag{B1}$$

where  $s = \pm$  for  $j = \pm$  and zero otherwise. The solution of these equations is obtained using the method of characteristics [62]. To employ this method, we first transform into the center-of-mass and relative coordinates  $R = (y + y')/2$  and  $r = y' - y$ . Then, we perform Fourier transform with respect to  $R$ :

$$\rho_j(R, r, t) = \frac{1}{\sqrt{2\pi}} \int_{-\infty}^{+\infty} dK e^{iKR} \rho_j(K, r, t). \tag{B2}$$



According to the method of characteristics, the solution for  $\rho_j(K, r, t)$  has the form

$$\rho_j(K, r, t) = \rho_j(K', r', 0)e^{aZ(K,r,t)+bZ'(K,r,t)-\frac{2i\sin Bt}{\hbar}}, \tag{B3}$$

where  $\rho_j(K', r', 0)$  is determined from the initial conditions. The other quantities that enter Eq. (B3) are defined as

$$a = \frac{\gamma}{2\beta m(\gamma^2 - \omega^2)}, \tag{B4}$$

$$b = \frac{\gamma\beta\hbar^2\omega^2}{32m(\gamma^2 - \omega^2)}, \tag{B5}$$

$$Z(K, r, t) = \frac{1}{\gamma}\left(K - \frac{r}{\lambda_+}\right)\left(K - \frac{r}{\lambda_-}\right)(1 - e^{-2\gamma t}) - \frac{m\lambda_+}{2\hbar}\left(K - \frac{r}{\lambda_+}\right)^2(1 - e^{-\frac{2\hbar t}{m\lambda_+}}) - \frac{m\lambda_-}{2\hbar}\left(K - \frac{r}{\lambda_-}\right)^2(1 - e^{-\frac{2\hbar t}{m\lambda_-}}), \tag{B6}$$

$$Z'(K, r, t) = \frac{1}{\gamma}\left(K - \frac{r}{\lambda_+}\right)\left(K - \frac{r}{\lambda_-}\right)(1 - e^{-2\gamma t}) - \frac{m^3\omega^2\lambda_+^3}{2\hbar^3}\left(K - \frac{r}{\lambda_+}\right)^2(1 - e^{-\frac{2\hbar t}{m\lambda_+}}) - \frac{m^3\omega^2\lambda_-^3}{2\hbar^3}\left(K - \frac{r}{\lambda_-}\right)^2(1 - e^{-\frac{2\hbar t}{m\lambda_-}}), \tag{B7}$$

$$\lambda_{\pm} = \frac{\hbar}{m\omega^2}(\gamma \pm \sqrt{\gamma^2 - \omega^2}), \tag{B8}$$

$$K' = \frac{(\lambda_+K - r)e^{-\frac{\hbar t}{m\lambda_+}} - (\lambda_-K - r)e^{-\frac{\hbar t}{m\lambda_-}}}{\lambda_+ - \lambda_-}, \tag{B9}$$

$$r' = \frac{\lambda_-(\lambda_+K - r)e^{-\frac{\hbar t}{m\lambda_+}} - \lambda_+(\lambda_-K - r)e^{-\frac{\hbar t}{m\lambda_-}}}{\lambda_+ - \lambda_-}. \tag{B10}$$

Notice that for  $B = 0$  this expression corresponds to the known solution of the Caldeira-Legett equation [62].

The initial condition Eq. (14) reads in  $K'$  and  $r'$  variables as follows:

$$\rho_0(K', r', 0) = \frac{1}{2\sqrt{2\pi}}e^{-\frac{K'^2 l_0^2}{4} - \frac{r'^2}{4l_0^2} - iK'y_0}; \tag{B11}$$

$\rho_3(K', r', 0) = p\rho_0(K', r', 0)$  and  $p = 1$  for spin polarized case and zero otherwise. For the sake of discussion, here we have also included  $y_0$ —the shift of the initial wave packet. The density matrix in real space is cumbersome. We do not present it here since in this paper we are not interested in spatial correlations. Instead, we focus on local observables for which  $y = y'$ ,  $R = y$  and  $r = 0$ . To calculate them, we note that  $K' = g_1(t)K$ ,  $r' = g_2(t)K$ ,  $Z(K, 0, t) = g_3(t)K^2$ ,  $Z'(K, 0, t) = g_4(t)K^2$ , where functions  $g_i(t)$  are defined as

$$g_1(t) = \frac{\lambda_+e^{-\frac{\hbar t}{m\lambda_+}} - \lambda_-e^{-\frac{\hbar t}{m\lambda_-}}}{\lambda_+ - \lambda_-}, \tag{B12}$$

$$g_2(t) = \frac{\lambda_+\lambda_-}{\lambda_+ - \lambda_-}(e^{-\frac{\hbar t}{m\lambda_+}} - e^{-\frac{\hbar t}{m\lambda_-}}), \tag{B13}$$

$$g_3(t) = \frac{1}{\gamma}(1 - e^{-2\gamma t}) - \frac{m\lambda_+}{2\hbar}(1 - e^{-\frac{2\hbar t}{m\lambda_+}}) - \frac{m\lambda_-}{2\hbar}(1 - e^{-\frac{2\hbar t}{m\lambda_-}}), \tag{B14}$$

$$g_4(t) = \frac{1}{\gamma}(1 - e^{-2\gamma t}) - \frac{m^3\omega^2\lambda_+^3}{2\hbar^3}(1 - e^{-\frac{2\hbar t}{m\lambda_+}}) - \frac{m^3\omega^2\lambda_-^3}{2\hbar^3}(1 - e^{-\frac{2\hbar t}{m\lambda_-}}). \tag{B15}$$

Now, we can compute the densities from Eq. (B3),

$$\rho_0(y, y, t) = \frac{1}{4\sqrt{\pi}b_0(t)}e^{-\frac{(y-y_0g_1(t))^2}{4b_0(t)}}, \tag{B16}$$

$$\rho_1(y, y, t) = p\rho_0(y, y, t)\sin\left(\frac{2\mu Bt}{\hbar}\right), \tag{B17}$$

$$\rho_2(y, y, t) = 0, \tag{B18}$$

$$\rho_3(y, y, t) = p\rho_0(y, y, t)\cos\left(\frac{2\mu Bt}{\hbar}\right), \tag{B19}$$

where  $b_0(t) = g_1^2(t)l_0^2/4 + g_2^2(t)/4l_0^2 - ag_3(t) - bg_4(t)$ . The typical observables can also be easily calculated:

$$\langle y \rangle = y_0g_1(t), \tag{B20}$$

$$\langle y^2 \rangle = y_0^2g_1^2(t) + 2b_0(t), \tag{B21}$$

$$\langle \sigma_x \rangle = p \sin \left( \frac{2\mu_B B t}{\hbar} \right), \tag{B22}$$

$$\langle y \sigma_x \rangle = p y_0 g_1(t) \sin \left( \frac{2\mu_B B t}{\hbar} \right), \tag{B23}$$

$$\langle \sigma_y \rangle = 0, \tag{B24}$$

$$\langle y \sigma_y \rangle = 0, \tag{B25}$$

$$\langle \sigma_z \rangle = p \cos \left( \frac{2\mu_B B t}{\hbar} \right), \tag{B26}$$

$$\langle y \sigma_z \rangle = p y_0 g_1(t) \cos \left( \frac{2\mu_B B t}{\hbar} \right). \tag{B27}$$

**2. Comparison with the fit used in the experiment**

In this section, we compare the result of Eq. (B21) with Eq. (10) of the main text, which we repeat here for convenience,

$$\bar{y} = \bar{y}_0 + \mathcal{A}_1 t - \mathcal{A}_2 e^{-\Gamma \Omega t} \cos[\sqrt{1 - \Gamma^2} \Omega(t - t_0)], \tag{B28}$$

where  $\bar{y} = \sqrt{\langle y^2 \rangle}$ . The functions  $g_i(t)$  that enter Eq. (B21) have the form

$$g_1(t) = \frac{\gamma e^{-\gamma t}}{\sqrt{\omega^2 - \gamma^2}} \sin(\sqrt{\omega^2 - \gamma^2} t) + e^{-\gamma t} \cos(\sqrt{\omega^2 - \gamma^2} t), \tag{B29}$$

$$g_2(t) = \frac{\hbar e^{-\gamma t}}{m \sqrt{\omega^2 - \gamma^2}} \sin(\sqrt{\omega^2 - \gamma^2} t), \tag{B30}$$

$$g_3(t) = \frac{\omega^2 - \gamma^2}{\gamma \omega^2} - \frac{1}{\gamma} e^{-2\gamma t} - \frac{\sqrt{\omega^2 - \gamma^2} e^{-2\gamma t}}{\omega^2} \sin(2\sqrt{\omega^2 - \gamma^2} t) + \frac{\gamma e^{-2\gamma t}}{\omega^2} \cos(2\sqrt{\omega^2 - \gamma^2} t), \tag{B31}$$

$$g_4(t) = \frac{\omega^4 - 4\gamma^4 + 3\gamma^2 \omega^2}{\gamma \omega^4} - \frac{1}{\gamma} e^{-2\gamma t} - \frac{(4\gamma^2 - \omega^2) \sqrt{\omega^2 - \gamma^2} e^{-2\gamma t}}{\omega^4} \sin(2\sqrt{\omega^2 - \gamma^2} t) + \frac{(4\gamma^3 - 3\gamma \omega^2) e^{-2\gamma t}}{\omega^4} \cos(2\sqrt{\omega^2 - \gamma^2} t). \tag{B32}$$

In the experiment,  $y_0 = 0$ ,  $\gamma \ll \omega$ , and  $k_B T \gg \hbar \omega$ , thus, we can ignore the effect of the minimally invasive term and approximate  $\langle y^2 \rangle$  as

$$\langle y^2 \rangle = 2b_0(t) \approx \frac{1}{2\beta m \omega^2} + \left( \frac{l_0^4 + l^4}{4l_0^2} - \frac{1}{2\beta m \omega^2} \right) e^{-2\gamma t} + \frac{l_0^4 - l^4}{4l_0^2} e^{-2\gamma t} \cos \left( 2\omega t \sqrt{1 - \left( \frac{\gamma}{\omega} \right)^2} \right). \tag{B33}$$

Note that in the experiment  $l_0$  is the smallest length scale, i.e.,  $l_0 \ll l$ , and that  $l^4/4l_0^2$  is comparable to  $1/2\beta m \omega^2$ . Therefore, at long times ( $t \gtrsim 1/\gamma$ ), we can estimate  $\langle y^2 \rangle$  by disregarding the exponentially decaying second term in Eq. (B33). After these simplifications, we derive

$$\langle y^2 \rangle \approx \frac{l^2}{2\beta \hbar \omega} - \frac{l^4}{4l_0^2} e^{-2\gamma t} \cos \left( 2\omega t \sqrt{1 - \left( \frac{\gamma}{\omega} \right)^2} \right). \tag{B34}$$

Comparing Eq. (B34) with Eq. (B28), we can identify  $\Omega = 2\omega$ ,  $\Gamma = \gamma/\omega$ ,  $\bar{y}_0 = l/\sqrt{2\beta \hbar \omega}$ ,  $\mathcal{A}_2 = l^4/8\bar{y}_0 l_0^2$ . We see that the dynamics of the system is fully determined by  $l_0$  and  $\gamma$ . Assuming that  $\gamma$  is measured in the experiment, the only free parameter is the initial energy fixed by  $l_0$ . Note that the width of the steady state does not depend on the initial state, in agreement with general postulates of thermodynamics.

The values of  $\mathcal{A}_1$  and  $t_0$  determine, in particular, the initial inflation, i.e., increase of the oscillation amplitude. These parameters describe phenomenologically the effect of exponentially decaying terms. Since they are strongly model dependent (i.e., depend on the choice of the fitting function), we do not discuss them here.

**3. Solution of the 1D master equation with  $B = 0$**

Here, we consider systems with  $\alpha \neq 0$  and  $B = 0$ . As was noted in the main text, in this case SOC can be gauged out by transformation

$$\rho(y, y', t) = e^{-\frac{i m \alpha x y}{\hbar}} f(y, y', t) e^{\frac{i m \alpha x y'}{\hbar}}, \tag{B35}$$

where  $f_s(y, y', t)$  satisfies Eq. (B1) with  $B = 0$ ; the function  $f$  has the form presented in Eq. (B3). The presence of SOC modifies the initial condition for  $f_j(K', r', 0)$ :

$$f_0(K', r', 0) = \cos\left(\frac{m\alpha r'}{\hbar}\right)\rho_0(K', r', 0), \quad (\text{B36})$$

$$f_1(K', r', 0) = -i \sin\left(\frac{m\alpha r'}{\hbar}\right)\rho_0(K', r', 0), \quad (\text{B37})$$

$$f_2(K', r', 0) = \frac{ip}{2}\left(e^{-\frac{m\alpha K'^2_0 + 2im\alpha y_0}{\hbar}} - e^{-\frac{m\alpha K'^2_0 + 2im\alpha y_0}{\hbar}}\right)e^{-\frac{m^2\alpha^2 l_0^2}{\hbar^2}}\rho_0(K', r', 0), \quad (\text{B38})$$

$$f_3(K', r', 0) = \frac{p}{2}\left(e^{-\frac{m\alpha K'^2_0 + 2im\alpha y_0}{\hbar}} + e^{-\frac{m\alpha K'^2_0 + 2im\alpha y_0}{\hbar}}\right)e^{-\frac{m^2\alpha^2 l_0^2}{\hbar^2}}\rho_0(K', r', 0). \quad (\text{B39})$$

From these density matrices, we can derive the densities via inverse Fourier transform:

$$f_0(y, y, t) = \frac{1}{8\sqrt{\pi}b_0(t)}\left(e^{-\frac{(y-y_0g_1(t)-\frac{m\alpha g_2(t)}{\hbar})^2}{4b_0(t)}} + e^{-\frac{(y-y_0g_1(t)+\frac{m\alpha g_2(t)}{\hbar})^2}{4b_0(t)}}\right), \quad (\text{B40})$$

$$f_1(y, y, t) = \frac{1}{8\sqrt{\pi}b_0(t)}\left(e^{-\frac{(y-y_0g_1(t)-\frac{m\alpha g_2(t)}{\hbar})^2}{4b_0(t)}} - e^{-\frac{(y-y_0g_1(t)+\frac{m\alpha g_2(t)}{\hbar})^2}{4b_0(t)}}\right), \quad (\text{B41})$$

$$f_2(y, y, t) = -\frac{ipe^{-\frac{m^2\alpha^2 l_0^2}{\hbar^2}}}{8\sqrt{\pi}b_0(t)}\left(e^{-\frac{2im\alpha y_0}{\hbar}}e^{-\frac{(y-y_0g_1(t)-\frac{im\alpha g_1(t)l_0^2}{\hbar})^2}{4b_0(t)}} - e^{-\frac{2im\alpha y_0}{\hbar}}e^{-\frac{(y-y_0g_1(t)+\frac{im\alpha g_1(t)l_0^2}{\hbar})^2}{4b_0(t)}}\right), \quad (\text{B42})$$

$$f_3(y, y, t) = \frac{pe^{-\frac{m^2\alpha^2 l_0^2}{\hbar^2}}}{8\sqrt{\pi}b_0(t)}\left(e^{-\frac{2im\alpha y_0}{\hbar}}e^{-\frac{(y-y_0g_1(t)-\frac{im\alpha g_1(t)l_0^2}{\hbar})^2}{4b_0(t)}} + e^{-\frac{2im\alpha y_0}{\hbar}}e^{-\frac{(y-y_0g_1(t)+\frac{im\alpha g_1(t)l_0^2}{\hbar})^2}{4b_0(t)}}\right). \quad (\text{B43})$$

After straightforward but tedious calculations, we derive time dynamics of observables

$$\langle y \rangle = y_0g_1(t), \quad (\text{B44})$$

$$\langle y^2 \rangle = y_0^2g_1^2(t) + 2b_0(t) + \frac{m^2\alpha^2g_2^2(t)}{\hbar^2}, \quad (\text{B45})$$

$$\langle \sigma_x \rangle = 0, \quad (\text{B46})$$

$$\langle y\sigma_x \rangle = \frac{m\alpha}{\hbar}g_2(t), \quad (\text{B47})$$

$$\langle \sigma_y \rangle = pe^{-\frac{m^2\alpha^2}{\hbar^2}(l_0^2(1+2g_1(t))-4b_0(t))}\sin\left(\frac{2m\alpha y_0}{\hbar}(1-g_1(t))\right), \quad (\text{B48})$$

$$\langle y\sigma_y \rangle = pe^{-\frac{m^2\alpha^2}{\hbar^2}(l_0^2(1+2g_1(t))-4b_0(t))}\left[\frac{m\alpha}{\hbar}(g_1(t)l_0^2 - 4b_0(t))\cos\left(\frac{2m\alpha y_0}{\hbar}(1-g_1(t))\right) - y_0g_1(t)\sin\left(\frac{2m\alpha y_0}{\hbar}(1-g_1(t))\right)\right], \quad (\text{B49})$$

$$\langle \sigma_z \rangle = pe^{-\frac{m^2\alpha^2}{\hbar^2}(l_0^2(1+2g_1(t))-4b_0(t))}\cos\left(\frac{2m\alpha y_0}{\hbar}(1-g_1(t))\right), \quad (\text{B50})$$

$$\langle y\sigma_z \rangle = pe^{-\frac{m^2\alpha^2}{\hbar^2}(l_0^2(1+2g_1(t))-4b_0(t))}\left[-\frac{m\alpha}{\hbar}(g_1(t)l_0^2 - 4b_0(t))\sin\left(\frac{2m\alpha y_0}{\hbar}(1-g_1(t))\right) + y_0g_1(t)\cos\left(\frac{2m\alpha y_0}{\hbar}(1-g_1(t))\right)\right]. \quad (\text{B51})$$

We see that the presence of SOC modifies the time dynamics of spin-independent observables, such as  $\langle y^2 \rangle$ . More importantly, it also generates spin dynamics, which was absent for  $\alpha = 0$ . To illustrate this dynamics, we consider  $\langle y\sigma_y \rangle$  assuming that the initial state is spin-polarized in the  $\mathbf{z}$ -direction (i.e.,  $p = 1$ ) and the initial packet is at the center of the well (i.e.,  $y_0 = 0$ ). According to Eq. (B49), SOC rotates the spin of the impurity, adding a component along the  $\mathbf{y}$  direction. This effect can be understood already at the level of a one-body Schrödinger equation. Presence of dissipation leads to a steady state for  $t \gg 1/\gamma$ . Indeed, in this case  $g_1(t) \rightarrow 0$  and  $g_2(t) \rightarrow 0$ , but  $g_3(t) \rightarrow (\omega^2 - \gamma^2)/(\omega^2\gamma)$  and  $g_4(t) \rightarrow (\omega^4 + 3\gamma^2\omega^2 - 4\gamma^4)/(\omega^4\gamma)$ , leading to a finite value of  $\langle y\sigma_y \rangle$  (see also the main text).

#### 4. Solution of the 1D master equation with $B \neq 0$ and $\alpha \neq 0$

Finally, we consider the case with finite magnetic fields and SOC, i.e.,  $B \neq 0$  and  $\alpha \neq 0$ . We perform the gauge transformation presented in Eq. (B35) and work with the function  $f$ . For the sake of discussion, we assume that the initial condition for  $f(y, y', t)$

is as for the  $B = 0$  case; we also assume that  $\mathbf{B} \parallel \mathbf{y}$ . Assuming that SOC is weak, we restrict our calculations to the first order in  $\alpha$ . The corresponding equations for  $f$  [ $f(y, y', t) = f_0\sigma_0 + f_1\sigma_x + f_2\sigma_y + f_3\sigma_z$ ] are

$$\frac{df_0}{dt} = \mathcal{L}f_0 + \frac{2i\mu_B B m \alpha}{\hbar^2} (y - y') f_3, \tag{B52}$$

$$\frac{df_1}{dt} = \mathcal{L}f_1 + \frac{2\mu_B B}{\hbar} f_3 + \frac{2\mu_B B m \alpha}{\hbar^2} (y + y') f_2, \tag{B53}$$

$$\frac{df_2}{dt} = \mathcal{L}f_2 - \frac{2\mu_B B m \alpha}{\hbar^2} (y + y') f_1, \tag{B54}$$

$$\frac{df_3}{dt} = \mathcal{L}f_3 - \frac{2\mu_B B}{\hbar} f_1 + \frac{2i\mu_B B m \alpha}{\hbar^2} (y - y') f_0, \tag{B55}$$

where  $\mathcal{L}$  is the operator that reproduces the right-hand side of the master equation with  $B = 0$  and  $\alpha = 0$ . From the initial conditions Eqs. (B36)–(B39), it is clear that  $f_2 \propto \alpha$  even when  $B = 0$ . Therefore, the last term of Eq. (B53) will be second order in  $\alpha$  and can be ignored. To proceed, we use the expansion  $f_i = f_i^0 + \alpha f_i^1$ , where  $f_i^0$  satisfies the equations with  $\alpha = 0$  [cf. Eq. (B3)]. Then, we solve the system of equations (it is convenient to solve for  $f_{\pm} = f_1 \pm i f_3$ ). For the densities in the leading order, we have

$$f_0^0(y, y, t) = f_0(y, y, t), \tag{B56}$$

$$f_1^0(y, y, t) = f_1(y, y, t) \cos\left(\frac{2\mu_B B t}{\hbar}\right) + f_3(y, y, t) \sin\left(\frac{2\mu_B B t}{\hbar}\right), \tag{B57}$$

$$f_2^0(y, y, t) = f_2(y, y, t), \tag{B58}$$

$$f_3^0(y, y, t) = -f_1(y, y, t) \sin\left(\frac{2\mu_B B t}{\hbar}\right) + f_3(y, y, t) \cos\left(\frac{2\mu_B B t}{\hbar}\right), \tag{B59}$$

where on the right-hand side we have density matrices from Eqs. (B40)–(B43). The corresponding functions  $f_i^1$  are

$$f_0^1(y, y, t) = \frac{2\mu_B B m}{\hbar^2} \text{Im} \left[ b_1(t) \frac{\partial}{\partial y} (f_1^0(y, y, t) - i f_3^0(y, y, t)) \right], \tag{B60}$$

$$f_1^1(y, y, t) = \frac{2\mu_B B m}{\hbar^2} \text{Im} \left[ b_1(t) \frac{\partial}{\partial y} f_0^0(y, y, t) \right], \tag{B61}$$

$$f_2^1(y, y, t) = -\frac{4\mu_B B m}{\hbar^2} \text{Re} \left[ b_2(t) \frac{\partial}{\partial y} (f_1^0(y, y, t) - i f_3^0(y, y, t)) \right] + \frac{4\mu_B B m y_0}{\hbar^2} f_1^0(y, y, t), \tag{B62}$$

$$f_3^1(y, y, t) = -\frac{2\mu_B B m}{\hbar^2} \text{Re} \left[ b_1(t) \frac{\partial}{\partial y} f_0^0(y, y, t) \right], \tag{B63}$$

where

$$b_1(t) = \frac{\frac{\hbar}{m} - \left(\frac{\hbar}{m} g_1(t) + \frac{2i\mu_B B}{\hbar} g_2(t)\right) e^{-\frac{2i\mu_B B t}{\hbar}}}{\omega^2 + \frac{4i\mu_B B \gamma}{\hbar} - \frac{4\mu_B^2 B^2}{\hbar^2}}, \tag{B64}$$

$$b_2(t) = \left( \frac{2a(\omega^2 - \gamma^2)}{\gamma\omega^2} + \frac{b(2\omega^4 + 6\gamma^2\omega^2 - 8\gamma^4)}{\gamma\omega^4} \right) \frac{(2\gamma + \frac{2i\mu_B B t}{\hbar}) \left(1 - g_1(t) e^{-\frac{2i\mu_B B t}{\hbar}}\right) + \frac{m\omega^2}{\hbar} g_2(t) e^{-\frac{2i\mu_B B t}{\hbar}}}{\omega^2 + \frac{4i\mu_B B \gamma}{\hbar} - \frac{4\mu_B^2 B^2}{\hbar^2}} - \frac{4mb(\omega^2 - \gamma^2)}{\hbar\omega^2} b_1(t) + \left[ \left( \frac{l_0^2}{2} + \frac{2a(\omega^2 - \gamma^2)}{\gamma\omega^2} + \frac{b(2\omega^4 + 6\gamma^2\omega^2 - 8\gamma^4)}{\gamma\omega^4} \right) g_1(t) - \frac{4mb(\omega^2 - \gamma^2)}{\hbar\omega^2} g_2(t) \right] g_5(t) + \left[ \left( \frac{1}{2l_0^2} + \frac{2(a+b)m^2(\omega^2 - \gamma^2)}{\hbar^2\gamma} \right) g_2(t) - \frac{4bm(\omega^2 - \gamma^2)}{\hbar\omega^2} g_1(t) \right] g_6(t), \tag{B65}$$

$$g_5(t) = \frac{1}{\lambda_+ - \lambda_-} \left( \lambda_+ \left( \frac{e^{-\frac{\hbar t}{m\lambda_+}} - e^{-\frac{2i\mu_B B t}{\hbar}}}{\frac{\hbar}{m\lambda_+} - \frac{2i\mu_B B}{\hbar}} \right) - \lambda_- \left( \frac{e^{-\frac{\hbar t}{m\lambda_-}} - e^{-\frac{2i\mu_B B t}{\hbar}}}{\frac{\hbar}{m\lambda_-} - \frac{2i\mu_B B}{\hbar}} \right) \right), \tag{B66}$$

$$g_6(t) = \frac{\lambda_+ \lambda_-}{\lambda_+ - \lambda_-} \left( \frac{e^{-\frac{\hbar t}{m\lambda_+}} - e^{-\frac{2i\mu_B B t}{\hbar}}}{\frac{\hbar}{m\lambda_+} - \frac{2i\mu_B B}{\hbar}} - \frac{e^{-\frac{\hbar t}{m\lambda_-}} - e^{-\frac{2i\mu_B B t}{\hbar}}}{\frac{\hbar}{m\lambda_-} - \frac{2i\mu_B B}{\hbar}} \right). \tag{B67}$$

The observables have the form

$$\langle y \rangle \approx y_0 g_1(t) + \frac{2p\alpha\mu_B B m}{\hbar^2} \text{Re}[b_1(t)e^{\frac{2i\mu_B B t}{\hbar}}], \quad (\text{B68})$$

$$\langle y^2 \rangle \approx y_0^2 g_1^2(t) + 2b_0(t) + \frac{4p\alpha\mu_B B m}{\hbar^2} y_0 g_1(t) \text{Re}[b_1(t)e^{\frac{2i\mu_B B t}{\hbar}}], \quad (\text{B69})$$

$$\langle \sigma_x \rangle \approx p \sin\left(\frac{2\mu_B B t}{\hbar}\right), \quad (\text{B70})$$

$$\langle y\sigma_x \rangle \approx \frac{m\alpha}{\hbar} g_2(t) \cos\left(\frac{2\mu_B B t}{\hbar}\right) + p y_0 g_1(t) \sin\left(\frac{2\mu_B B t}{\hbar}\right) - \frac{2\alpha\mu_B B m}{\hbar^2} \text{Im}[b_1(t)], \quad (\text{B71})$$

$$\langle \sigma_y \rangle \approx \frac{2pm\alpha y_0}{\hbar} (1 - g_1(t)), \quad (\text{B72})$$

$$\langle y\sigma_y \rangle \approx \frac{pm\alpha}{\hbar} g_1(t) (l_0^2 + 2y_0^2) - \frac{pm\alpha}{\hbar} \left[ g_1^2(t) (l_0^2 + 2y_0^2) + \frac{g_2^2(t)}{l_0^2} - 4(ag_3(t) + bg_4(t)) \right] \\ \times \cos\left(\frac{2\mu_B B t}{\hbar}\right) + \frac{4p\alpha\mu_B B m}{\hbar^2} \text{Im}[b_2 e^{\frac{2i\mu_B B t}{\hbar}}] + \frac{4p\alpha\mu_B B m y_0^2}{\hbar^2} g_1(t) \sin\left(\frac{2\mu_B B t}{\hbar}\right), \quad (\text{B73})$$

$$\langle \sigma_z \rangle \approx p \cos\left(\frac{2\mu_B B t}{\hbar}\right), \quad (\text{B74})$$

$$\langle y\sigma_z \rangle \approx p y_0 g_1(t) \cos\left(\frac{2\mu_B B t}{\hbar}\right) - \frac{m\alpha}{\hbar} g_2(t) \sin\left(\frac{2\mu_B B t}{\hbar}\right) + \frac{2\alpha\mu_B B m}{\hbar^2} \text{Re}[b_1(t)]. \quad (\text{B75})$$

We checked numerically that these expressions are accurate for small values of  $\alpha$ , and off-resonant magnetic fields. (The resonance is located at  $\hbar\omega = 2\mu_B B$ .)

- 
- [1] A. McDonald, T. Pereg-Barnea, and A. A. Clerk, Phase-Dependent Chiral Transport and Effective Non-Hermitian Dynamics in a Bosonic Kitaev-Majorana Chain, *Phys. Rev. X* **8**, 041031 (2018).
- [2] V. P. Flynn, E. Cobanera, and L. Viola, Topology by Dissipation: Majorana Bosons in Metastable Quadratic Markovian Dynamics, *Phys. Rev. Lett.* **127**, 245701 (2021).
- [3] C.-X. Liu, J. D. Sau, and S. Das Sarma, Role of dissipation in realistic Majorana nanowires, *Phys. Rev. B* **95**, 054502 (2017).
- [4] Y. Huang, A. M. Lobos, and Z. Cai, Dissipative Majorana quantum wires, *iScience* **21**, 241 (2019).
- [5] A. Kavokin, G. Malpuech, and M. Glazov, Optical Spin Hall Effect, *Phys. Rev. Lett.* **95**, 136601 (2005).
- [6] C. Leyder, M. Romanelli, J. P. Karr, E. Giacobino, T. C. Liew, M. M. Glazov, A. V. Kavokin, G. Malpuech, and A. Bramati, Observation of the optical spin Hall effect, *Nat. Phys.* **3**, 628 (2007).
- [7] R. Naaman, Y. Paltiel, and D. Waldeck, Chiral molecules and the electron spin, *Nat. Rev. Chem.* **3**, 250 (2019).
- [8] F. Evers, A. Aharony, N. Bar-Gill, O. Entin-Wohlman, P. Hedegård, O. Hod, P. Jelinek, G. Kamieniarz, M. Lemeshko, K. Michaeli, V. Mujica, R. Naaman, Y. Paltiel, S. Refaely-Abramson, O. Tal, J. Thijssen, M. Thoss, J. M. van Ruitenbeek, L. Venkataraman, D. H. Waldeck *et al.*, Theory of chirality induced spin selectivity: Progress and challenges, *Adv. Mater.* **34**, 2106629 (2022).
- [9] T. Langen, R. Geiger, and J. Schmiedmayer, Ultracold atoms out of equilibrium, *Annu. Rev. Condens. Matter Phys.* **6**, 201 (2015).
- [10] A. Polkovnikov, K. Sengupta, A. Silva, and M. Vengalattore, Colloquium: Nonequilibrium dynamics of closed interacting quantum systems, *Rev. Mod. Phys.* **83**, 863 (2011).
- [11] L. D'Alessio, Y. Kafri, A. Polkovnikov, and M. Rigol, From quantum chaos and eigenstate thermalization to statistical mechanics and thermodynamics, *Adv. Phys.* **65**, 239 (2016).
- [12] R. J. Lewis-Swan, A. Safavi-Naini, A. M. Kaufman, and A. M. Rey, Dynamics of quantum information, *Nat. Rev. Phys.* **1**, 627 (2019).
- [13] D. A. Abanin, E. Altman, I. Bloch, and M. Serbyn, Colloquium: Many-body localization, thermalization, and entanglement, *Rev. Mod. Phys.* **91**, 021001 (2019).
- [14] J. Dalibard, F. Gerbier, G. Juzeliūnas, and P. Öhberg, Colloquium: Artificial gauge potentials for neutral atoms, *Rev. Mod. Phys.* **83**, 1523 (2011).
- [15] V. Galitski and I. B. Spielman, Spin-orbit coupling in quantum gases, *Nature (London)* **494**, 49 (2013).
- [16] E. Altman, K. R. Brown, G. Carleo, L. D. Carr, E. Demler, C. Chin, B. DeMarco, S. E. Economou, M. A. Eriksson, K.-M. C. Fu, M. Greiner, K. R. A. Hazzard, R. G. Hulet, A. J. Kollár, B. L. Lev, M. D. Lukin, R. Ma, X. Mi, S. Misra, C. Monroe *et al.*, Quantum simulators: Architectures and opportunities, *PRX Quantum* **2**, 017003 (2021).
- [17] T. Hata, E. Nakano, K. Iida, H. Tajima, and J. Takahashi, Dissipation-relaxation dynamics of a spin- $\frac{1}{2}$  particle with a Rashba-type spin-orbit coupling in an ohmic heat bath, *Phys. Rev. B* **104**, 144424 (2021).
- [18] A. Caldeira and A. Leggett, Path integral approach to quantum Brownian motion, *Physica A* **121**, 587 (1983).
- [19] H.-P. Breuer, and F. Petruccione, *The Theory of Open Quantum Systems* (Oxford University Press, Oxford, UK, 2002).
- [20] J. Catani, G. Lamporesi, D. Naik, M. Gring, M. Inguscio, F. Minardi, A. Kantian, and T. Giamarchi, Quantum dynamics of impurities in a one-dimensional Bose gas, *Phys. Rev. A* **85**, 023623 (2012).

- [21] F. Grusdt, G. E. Astrakharchik, and E. Demler, Bose polarons in ultracold atoms in one dimension: Beyond the Fröhlich paradigm, *New J. Phys.* **19**, 103035 (2017).
- [22] A. O. Caldeira, *An Introduction to Macroscopic Quantum Phenomena and Quantum Dissipation* (University Printing House, Cambridge, United Kingdom, 2014).
- [23] A. Lampo, S. H. Lim, M. Á. García-March, and M. Lewenstein, Bose polaron as an instance of quantum Brownian motion, *Quantum* **1**, 30 (2017).
- [24] A. Recati, P. O. Fedichev, W. Zwerger, J. von Delft, and P. Zoller, Atomic Quantum Dots Coupled to a Reservoir of a Superfluid Bose-Einstein Condensate, *Phys. Rev. Lett.* **94**, 040404 (2005).
- [25] A. Caldeira and A. Leggett, Quantum tunnelling in a dissipative system, *Ann. Phys.* **149**, 374 (1983).
- [26] P. Massignan, M. Zaccanti, and G. M. Bruun, Polarons, dressed molecules and itinerant ferromagnetism in ultracold Fermi gases, *Rep. Prog. Phys.* **77**, 034401 (2014).
- [27] F. Chevy and C. Mora, Ultra-cold polarized Fermi gases, *Rep. Prog. Phys.* **73**, 112401 (2010).
- [28] F. Grusdt and E. Demler, New theoretical approaches to Bose polarons, *Quantum Matter Ultralow Temp.* **191**, 325 (2015).
- [29] F. Scazza, M. Zaccanti, P. Massignan, M. M. Parish, and J. Levinsen, Repulsive Fermi and Bose polarons in quantum gases, *Atoms* **10**, 55 (2022).
- [30] R. Schmidt, M. Knap, D. A. Ivanov, J.-S. You, M. Cetina, and E. Demler, Universal many-body response of heavy impurities coupled to a Fermi sea: A review of recent progress, *Rep. Prog. Phys.* **81**, 024401 (2018).
- [31] A. Schirotzek, C.-H. Wu, A. Sommer, and M. W. Zwierlein, Observation of Fermi Polarons in a Tunable Fermi Liquid of Ultracold Atoms, *Phys. Rev. Lett.* **102**, 230402 (2009).
- [32] M. Koschorreck, D. Pertot, E. Vogt, B. Fröhlich, M. Feld, and M. Köhl, Attractive and repulsive Fermi polarons in two dimensions, *Nature (London)* **485**, 619 (2012).
- [33] M. Cetina, M. Jag, R. S. Lous, I. Fritsche, J. T. Walraven, R. Grimm, J. Levinsen, M. M. Parish, R. Schmidt, M. Knap, and E. Demler, Ultrafast many-body interferometry of impurities coupled to a Fermi sea, *Science* **354**, 96 (2016).
- [34] F. Scazza, G. Valtolina, P. Massignan, A. Recati, A. Amico, A. Burchianti, C. Fort, M. Inguscio, M. Zaccanti, and G. Roati, Repulsive Fermi Polarons in a Resonant Mixture of Ultracold  ${}^6\text{Li}$  Atoms, *Phys. Rev. Lett.* **118**, 083602 (2017).
- [35] N. Spethmann, F. Kindermann, S. John, C. Weber, D. Meschede, and A. Widera, Dynamics of Single Neutral Impurity Atoms Immersed in an Ultracold Gas, *Phys. Rev. Lett.* **109**, 235301 (2012).
- [36] M.-G. Hu, M. J. Van de Graaff, D. Kedar, J. P. Corson, E. A. Cornell, and D. S. Jin, Bose Polarons in the Strongly Interacting Regime, *Phys. Rev. Lett.* **117**, 055301 (2016).
- [37] N. B. Jørgensen, L. Wacker, K. T. Skalmstang, M. M. Parish, J. Levinsen, R. S. Christensen, G. M. Bruun, and J. J. Arlt, Observation of Attractive and Repulsive Polarons in a Bose-Einstein Condensate, *Phys. Rev. Lett.* **117**, 055302 (2016).
- [38] Z. Z. Yan, Y. Ni, C. Robens, and M. W. Zwierlein, Bose polarons near quantum criticality, *Science* **368**, 190 (2020).
- [39] M. G. Skou, T. G. Skov, N. B. Jørgensen, K. K. Nielsen, A. Camacho-Guardian, T. Pohl, G. M. Bruun, and J. J. Arlt, Non-equilibrium quantum dynamics and formation of the Bose polaron, *Nat. Phys.* **17**, 731 (2021).
- [40] A. G. Volosniev, H.-W. Hammer, and N. T. Zinner, Real-time dynamics of an impurity in an ideal Bose gas in a trap, *Phys. Rev. A* **92**, 023623 (2015).
- [41] Y. E. Shchadilova, R. Schmidt, F. Grusdt, and E. Demler, Quantum Dynamics of Ultracold Bose Polarons, *Phys. Rev. Lett.* **117**, 113002 (2016).
- [42] M. Drescher, M. Salmhofer, and T. Enss, Real-space dynamics of attractive and repulsive polarons in Bose-Einstein condensates, *Phys. Rev. A* **99**, 023601 (2019).
- [43] D. Dzsojtjan, R. Schmidt, and M. Fleischhauer, Dynamical Variational Approach to Bose Polarons at Finite Temperatures, *Phys. Rev. Lett.* **124**, 223401 (2020).
- [44] S. Peotta, D. Rossini, M. Polini, F. Minardi, and R. Fazio, Quantum Breathing of an Impurity in a One-Dimensional Bath of Interacting Bosons, *Phys. Rev. Lett.* **110**, 015302 (2013).
- [45] S. I. Mistakidis, G. C. Katsimiga, G. M. Koutentakis, T. Busch, and P. Schmelcher, Quench Dynamics and Orthogonality Catastrophe of Bose Polarons, *Phys. Rev. Lett.* **122**, 183001 (2019).
- [46] S. I. Mistakidis, A. G. Volosniev, R. E. Barfknecht, T. Fogarty, T. Busch, A. Foerster, P. Schmelcher, and N. T. Zinner, Cold atoms in low dimensions—a laboratory for quantum dynamics, [arXiv:2202.11071](https://arxiv.org/abs/2202.11071).
- [47] P. Massignan, A. Lampo, J. Wehr, and M. Lewenstein, Quantum Brownian motion with inhomogeneous damping and diffusion, *Phys. Rev. A* **91**, 033627 (2015).
- [48] A. Lampo, C. Charalambous, M. A. García-March, and M. Lewenstein, Non-Markovian polaron dynamics in a trapped Bose-Einstein condensate, *Phys. Rev. A* **98**, 063630 (2018).
- [49] K. K. Nielsen, L. A. P. Ardila, G. M. Bruun, and T. Pohl, Critical slowdown of non-equilibrium polaron dynamics, *New J. Phys.* **21**, 043014 (2019).
- [50] M. Le Bellac, *Non Equilibrium Statistical Mechanics* (Les Houches Predoctoral School, 2007).
- [51] C. Gardiner and P. Zoller, *Quantum Noise: A Handbook of Markovian and Non-Markovian Quantum Stochastic Methods with Applications to Quantum Optics*, Springer Series in Synergetics (Springer Berlin, Heidelberg, 2004).
- [52] A. J. Leggett, S. Chakravarty, A. T. Dorsey, M. P. A. Fisher, A. Garg, and W. Zwerger, Dynamics of the dissipative two-state system, *Rev. Mod. Phys.* **59**, 1 (1987).
- [53] L. Henriot and K. Le Hur, Quantum sweeps, synchronization, and Kibble-Zurek physics in dissipative quantum spin systems, *Phys. Rev. B* **93**, 064411 (2016).
- [54] P. P. Orth, I. Stanic, and K. Le Hur, Dissipative quantum Ising model in a cold-atom spin-boson mixture, *Phys. Rev. A* **77**, 051601(R) (2008).
- [55] D. Dalidovich and M. P. Kennett, Bose-hubbard model in the presence of ohmic dissipation, *Phys. Rev. A* **79**, 053611 (2009).
- [56] V. Popov, J. Niederle, and L. Hlavatý, *Functional Integrals in Quantum Field Theory and Statistical Physics*, Mathematical Physics and Applied Mathematics (Springer, Netherlands, 2001).
- [57] L. Ferialdi, Dissipation in the Caldeira-Leggett model, *Phys. Rev. A* **95**, 052109 (2017).
- [58] S. I. Mistakidis, A. G. Volosniev, N. T. Zinner, and P. Schmelcher, Effective approach to impurity dynamics in

- one-dimensional trapped Bose gases, *Phys. Rev. A* **100**, 013619 (2019).
- [59] J. Jäger, R. Barnett, M. Will, and M. Fleischhauer, Strong-coupling Bose polarons in one dimension: Condensate deformation and modified Bogoliubov phonons, *Phys. Rev. Res.* **2**, 033142 (2020).
- [60] A. Alexandrov and J. Devreese, *Advances in Polaron Physics* (Springer, Berlin, 2009).
- [61] T. H. Johnson, M. Bruderer, Y. Cai, S. R. Clark, W. Bao, and D. Jaksch, Breathing oscillations of a trapped impurity in a Bose gas, *Europhys. Lett.* **98**, 26001 (2012).
- [62] S. Roy and A. Venugopalan, Exact solutions of the Caldeira-Leggett master equation: a factorization theorem for decoherence, [arXiv:quant-ph/9910004](https://arxiv.org/abs/quant-ph/9910004).
- [63] E. C. Zachmanoglou and D. W. Thoe, *Introduction to Partial Differential Equations with Applications* (Williams & Wilkins, Baltimore, 1976), pp. 112–152.
- [64] We checked that  $\gamma$  could be even fixed to the central value reported in the experiment, without affecting much the quality of the fit.
- [65] The accuracy of the fit could be slightly improved by allowing the temperature to vary within the experimental error bars. We do not do it here to avoid having an additional fitting parameter.
- [66] In this interpretation, the initial state is given by the polaron described by the Hamiltonian  $-\frac{\hbar^2}{2m_p} \frac{\partial^2}{\partial y^2} + \frac{m\omega_{\text{SSDP}}^2 y^2}{2}$ . At  $t > 0$ , the polaron is destroyed, which can be due to the anomalous behavior of the residue [83] or a highly nonequilibrium nature of the problem (cf. Ref. [84]). To show the existence of the polaron at  $t = 0$ , one needs to consider ground-state properties of an impurity in a tight trap—hence with a high kinetic energy—which is beyond the scope of the present work.
- [67] Here, we calculate the expectation value of the kinetic energy for a free particle described by the Gaussian wave packet:  $-\frac{\hbar^2}{2m} \langle \frac{\partial^2}{\partial y^2} \rangle$ , and relate it to  $\hbar\omega_{\text{SSDP}} \sqrt{m/m_p}$ , which is the typical energy scale of the polaron Hamiltonian:  $-\frac{\hbar^2}{2m_p} \frac{\partial^2}{\partial y^2} + \frac{m\omega_{\text{SSDP}}^2 y^2}{2}$ .
- [68] L. Parisi and S. Giorgini, Quantum Monte Carlo study of the Bose-polaron problem in a one-dimensional gas with contact interactions, *Phys. Rev. A* **95**, 023619 (2017).
- [69] G. Panochko and V. Pastukhov, Mean-field construction for spectrum of one-dimensional Bose polaron, *Ann. Phys.* **409**, 167933 (2019).
- [70] One expects that large values of  $\eta$  require a beyond-linear-coupling treatment of impurity-bath interactions [21,85], which is beyond the scope of the present paper.
- [71] A. S. Dehkharghani, A. G. Volosniev, and N. T. Zinner, Quantum impurity in a one-dimensional trapped Bose gas, *Phys. Rev. A* **92**, 031601(R) (2015).
- [72] M. Schechter, D. M. Gangardt, and A. Kamenev, Quantum impurities: From mobile Josephson junctions to depletions, *New J. Phys.* **18**, 065002 (2016).
- [73] J. Struck, J. Simonet, and K. Sengstock, Spin-orbit coupling in periodically driven optical lattices, *Phys. Rev. A* **90**, 031601(R) (2014).
- [74] X. Luo, L. Wu, J. Chen, Q. Guan, K. Gao, Z.-F. Xu, L. You, and R. Wang, Tunable atomic spin-orbit coupling synthesized with a modulating gradient magnetic field, *Sci. Rep.* **6**, 18983 (2016).
- [75] B. Shteynas, J. Lee, F. C. Top, J.-R. Li, A. O. Jamison, G. Juzeliūnas, and W. Ketterle, How to Dress Radio-Frequency Photons with Tunable Momentum, *Phys. Rev. Lett.* **123**, 033203 (2019).
- [76] A.-M. Guo and Q.-f. Sun, Spin-Selective Transport of Electrons in DNA Double Helix, *Phys. Rev. Lett.* **108**, 218102 (2012).
- [77] J. Fransson, Vibrational origin of exchange splitting and chiral-induced spin selectivity, *Phys. Rev. B* **102**, 235416 (2020).
- [78] Y. Liu, J. Xiao, J. Koo, and B. Yan, Chirality-driven topological electronic structure of dna-like materials, *Nat. Mater.* **20**, 638 (2021).
- [79] A. G. Volosniev, H. Alpern, Y. Paltiel, O. Millo, M. Lemesko, and A. Ghazaryan, Interplay between friction and spin-orbit coupling as a source of spin polarization, *Phys. Rev. B* **104**, 024430 (2021).
- [80] J. Fransson, Charge redistribution and spin polarization driven by correlation induced electron exchange in chiral molecules, *Nano Lett.* **21**, 3026 (2021).
- [81] M. Barroso, J. Balduque, F. Domínguez-Adame, and E. Díaz, Spin-dependent polaron transport in helical molecules, *Appl. Phys. Lett.* **121**, 143505 (2022).
- [82] This would require to consider higher spatial dimensions as our results suggest that relevant effects due to SOC can be gauged out in 1D.
- [83] V. Pastukhov, Impurity states in the one-dimensional Bose gas, *Phys. Rev. A* **96**, 043625 (2017).
- [84] G. M. Koutentakis, S. I. Mistakidis, and P. Schmelcher, Pattern formation in one-dimensional polaron systems and temporal orthogonality catastrophe, *Atoms* **10**, 3 (2022).
- [85] B. Kain and H. Y. Ling, Analytical study of static beyond-Fröhlich Bose polarons in one dimension, *Phys. Rev. A* **98**, 033610 (2018).